A technical pipeline for screening microbial communities as a function of substrate specificity through single cell fluorescent imaging

Shaun Leivers [a]#, Leidy Lagos [b]*, Sabina Leanti La Rosa [a,b], Bjørge Westereng [a]#

[a]Faculty of Chemistry, Biotechnology and Food Science, Norwegian University of Life Sciences, Aas, Norway.

[b]Faculty of Biosciences, Norwegian University of Life Sciences, Aas, Norway.

***Present address**: Leidy Lagos, Skretting ARC, Stavanger, Norway

Corresponding Authors

Dr S Leivers# E-mail: shaun.allan.leivers@nmbu.no.

Dr B Westereng# E-mail: bjorge.westereng@nmbu.no.

Running title: Screening microbial consortia by fluorescent labelling

Word count

Abstract: 167 Importance: 126

Text: 3246 (Excluding Materials and Methods)

ABSTRACT:

The study of specific glycan uptake and metabolism has been shown to be an effective tool in aiding with the continued unravelling of the complexities in the human gut microbiome. To this aim fluorescent labelling of glycans may provide a powerful route towards target. In this study,

we successfully used the fluorescent label 2-aminobenzamide (2-AB), most commonly employed for enhancing the detection of protein anchored glycans, to monitor and study microbial degradation of labelled glycans. Both single strain and co-cultured fermentations of microbes from the common human-gut derived Bacteroides genus, were able to grow when supplemented with 2-AB labelled glycans of different monosaccharide composition, degrees of acetylation and polymerization. Utilizing a multifaceted approach that combines chromatography, mass spectrometry, microscopy and flow cytometry techniques, it was possible to comprehensively track the metabolism of the labelled glycans in both supernatants and at a single cell level. We envisage this combination of complimentary techniques will help further the understanding of substrate specificity and the role it plays within microbial communities.

IMPORTANCE:

Information on how bacterial consortia utilize polysaccharides at strain level, whilst progressing rapidly in recent years still lacks a suitable way to study the vast range of ornamentations and structural motifs found in the natural glycans we consume in everyday life. As multi-omic approaches commonly require complex and costly analysis, a screening platform, as described in our work, could be seen as both a complementary and essential new tool in the understanding of microbial polysaccharide metabolism. Our study demonstrates a fast and efficient glycan labelling technique composed of several integrated procedures and advanced analytical methodologies. Chromatography and mass spectrometry are applied in the tracking of metabolized labelled glycans whilst microscopy and flow cytometry are used in the visualization of labelled bacteria at a single cell level.

INTRODUCTION

The Complexity of the Human Gut Microbiome. The study of interactions between carbohydrates and bacteria has long been highlighted as crucial to understanding the genetic diversity of microbial communities present within the human gastrointestinal tract (GIT)(1). In turn, this information helps us further our knowledge of how modifications within diet, through a subsequent change in glycan uptake and utilization, may impact on the gut microbiome(2). Previous studies have emphasized the importance of a symbiotic environment(3) and discussed competition and cooperation(4) behaviors in the human gut microbiome. Whilst a number of known beneficial members of the gut, particularly those belonging to *Lactobacillus* and *Bifidobacterium* spp., have been routinely studied with regards to uptake and metabolism of simpler glycans in recent years(5) (6), those assigned to the genus *Bacteroides*, which accounts for ~25% of bacterial cells in the human intestine(7), have only more recently garnered such attention for their capability to utilize complex glycans(8) (9). The possibility to develop complex prebiotic glycans to selectively engage beneficial microbes rests on understanding substrate selectivity as bacteria have developed highly specialized mechanisms for catabolizing the vast ensemble of glycan structures and their associated motifs(10) (11).

Catabolism and Utilization of Glycans. Members of the Bacteroidetes phylum are renowned for their abilities to degrade a wide range of glycans available through diet, host secretions, microbial exopolysaccharides and capsules(9). Within Bacteroidetes, *Bacteroides* dedicate a substantial proportion of their genome to carbohydrate active enzymes (CAZymes)(12) Sequencing of the *B. thetaiotaomicron* (*B. theta*) genome(13) along with the discovery of the architecture of polysaccharide utilization loci (PULs)(14), by which the Bacteroidetes phyla

depolymerize and degrade complex glycans, opened the door for further understanding of the degradation mechanisms(15) of glycans in the gut(16). The first PUL that was identified and fully characterized was the *B. theta* Starch utilization system (Sus), which consists of eight genes (*susRABCDEFG*) coding for proteins involved in the sensing, capture, uptake and hydrolysis of starch(17). The Sus has been used as an archetype for understanding other PUL systems and the nomenclature used to refer to the Sus is the convention when describing other loci. Despite variations in the glycan they target, PULs are defined by the presence of so-called SusC-like and SusD-like genes, encoding an outer membrane TonB-dependent transporter and a binding protein, respectively. SusCD-like complexes have been shown to mediate substrate uptake via a "pedal bin" transport mechanism, where SusC forms the barrel of the bin and the SusD-like protein acts as a lid on top of the barrel, opening and closing to facilitate substrate binding(18). A few studies have reported that SusCD transporters have a size limit for substrate transport, indicating that ~5 kDa may be a general total size limit for these systems(19) (18) (20). More recently, several PULs systems from other phyla such as Firmicutes and Bifidobacteria have been studied in detail(21) (22) (23). Whilst a wealth of knowledge is available regarding the individual strain-based degradation processes involved in complex glycan catabolism (24) (25), the effect of competitive environments faced by bacteria, despite recent advances in the field(26) (27), is poorly understood. With this in mind, a set of fast and effective tools for screening and testing different substrates to identify which bacteria within a community are capable of catabolizing them is of great interest.

Exploring Glycan-Microbial Consortia Interactions. Interspecies competition between *Bacteroides* spp. has been studied in mice fed "microbiota directed foods" (or MDF, through bead-based labelling) (27). Such data has thus far enhanced the understanding and potential for therapeutic targeting of beneficial human gut bacteria through the use of prebiotic introductions(28). Labelling of *B. fragilis* using 'metabolic oligosaccharide engineering (MOE) and biorthogonal click chemistry (BCC)' – used *in vivo* to observe host-commensal interactions in the intestine were able to further label and resolve mixed bacterial species including *B. vulgatus, B. ovatus* & *B. theta*(29). The deletion of specific pathways for degradation and transport of certain glycans PULs(30) as well as identifying the storage of labels within certain cells(31) was investigated through fluorescent labelling of cells, specifically utilizing epifluorescence microscopy and superresolution structured illumination microscopy (SR-SIM). *B. cellulosilyticus* WH2 along with *B. caccae*, *B. ovatus* & *B. theta* have been used to explore symbiotic relationships in the gut, focused mainly around xylan utilization(32). Discrete chemical structure variation can be employed as a directive influence on gut microbiome short chain fatty acid (SCFA) production whilst microbiome-modulating strategies based on variation in fine structure of carbohydrates were found to confer a selective enrichment of a specific number of bacterial taxa(33). The application of dietary carbohydrates in relation to food composition, gut microbiota and metabolic outputs as well as the interaction and utilization of functional groups is key to unravelling this complex community(34) (35) (36).

Emerging Fluorescence Labelling Techniques & Strategies. Fluorescent labelling of substrates is a valuable tool in furthering the understanding of the glycobiome(37). The importance and

impact of substrate decoration and the relationship to selectivity has been explored through systematic depolymerization and labelling of carbohydrates such as *β*-glucans(38), xylan (39) cellulose(40) and complex *N*-glycans (CNG)(25). Applications of fluorescently labelled substrates have allowed for the study into the uptake and utilization of polysaccharides in marine microbial communities(31) (41) (42). However, the overwhelming majority of these studies employ a bulky and expensive fluorescein-based derivative such as fluorescein isothiocyanate (FITC)(37), fluorescein-5-thiosemicarbazide (FTSC)(43) or fluorescein amidite (FAM) as the fluorescent component. Despite extensive reviews into the capabilities of a multitude of readily available fluorescent glycoconjugates(44) (45) (46) (47), the experimental pool of studies which use a non-fluorescein based alternative label in microbiome analysis is still limited, with the exception of 2-(*N*-(7-Nitrobenz-2-oxa-1,3-diazol-4-yl)Amino)-2-Deoxyglucose (2-NBDGlucose) which is routinely used for cell tracking in yeast(48) (49) and *Escherichia coli*(50) , and more recently in the analysis of the uncultured rumen microbiome(51).

Despite the evident potential for implementing glycan labelling as a tool for microbial exploration, the focus has mainly, in terms of identification and quantification(52) been on enhancing chromatographic techniques, specifically high performance liquid chromatography (HPLC)-ultra violet (UV)(53) and HPLC-fluorescence detection (FLD)(54). In relation to efficient separation, HILIC columns have proved useful for analyzing fluorescently labelled glycans, providing high selectivity for complex oligosaccharides(55) (56). When analyzing labelled carbohydrates mass spectrometry (MS) or comparable hyphenated techniques (LCMS) have provided an effective platform for the elucidation of complex, structurally highly similar complex glycans(57) (58) (59). Flow cytometry has emerged as a powerful tool to disseminate

labelled cells by fluorescence-activated cell sorting (FACS)(51). Fluorescently labelled glycans used in microbial fermentation experiments have been observed through a variety of microscopy techniques, particularly epifluorescence in combination with more detailed studies by confocal microscopy(31) (30).

A New Approach for Microbial Screening – Smaller, Faster, Cheaper. Use of small aromatic fluorophores has commonly and successfully been applied in glycosylation studies(60, 61), to enable effective analytical glycan detection. Two such readily used are 2-aminobenzoic acid (2-AA) and 2-aminobenzamide (2-AB). These labels are added to glycans via reductive amination(62), although these methods have often included a number of drawbacks such as the use of CN containing reducing agents as well as using dimethyl sulfoxide (DMSO) as the reaction medium. Due to its high toxicity, eliminating residual cyanide in products is essential when utilizing labelled glycans in microbial fermentations. More recently, alternative methodologies using 2-Picoline-borane (pic-BH_3) in one pot reductive aminations in methanol, water and solvent free conditions have been explored(63). Comparisons and potential benefits of pic-BH_3 based reactions over more traditional $NaCNBH_3$ have also been extensively demonstrated(64) (65) (66). Many glycans have non-carbohydrate motifs, such as acetylations, phosphate-, sulphate- or methyl- groups that are potentially vulnerable to pH extremes. Choosing benign labelling conditions which allow such substituents to remain intact after conjugation is thus of key importance. Smaller fluorescent compounds like 2-AB may affect binding and transport to a lesser extent than more bulky fluorophores, thus potentially providing a sensible complementary alternative to fluorescein-based derivatives for labelling. Here we look to introduce a simple, efficient and cheap alternative use of the fluorescent label 2-AB to be

154 utilized as a tool for monitoring glycan uptake in relation to bacterial substrate specificity. The
155 procedure is both substituent benign and utilizes non-toxic reagents that ensure substrates are
156 readily accessible in a biological context. We also present a comprehensive analytical approach
157 that warrants highly sensitive, routine HPLC principles combined with FACS and high-resolution
158 microscopy.

159 **RESULTS AND DISCUSSION**

160 Many glycan labelling techniques used for biological visualisation purposes focus on large, bulky
161 multi-ring moieties. In contrast, fluorescent labels used to compensate for a carbohydrates lack
162 of natural chromophore in analytical, specifically chromatographic applications, are often
163 smaller and subsequently less complex. Particularly important for practical applications, these
164 labels are often cheaper and can be more readily analytically identified than labels/dyes
165 produced specifically for biological applications. However, whilst structurally larger fluorescent
166 labels such as fluorescein or pyrene/anthracene-derived compounds have also been used for
167 chromatographic applications, conversely smaller labels, such as 2-AB, have not been routinely
168 utilized when studying biological environments.

169 **Substrate generation & Characterisation.** In this study we used reducing end coupling by
170 reductive amination (via picoline borane) to successfully conjugate 2-AB molecules to β-
171 mannan- and xylan-derived oligosaccharides from Norway spruce and birch wood (Fig.1 A). The
172 labelled products were subsequently detected and differentiated by HPLC hydrophilic
173 interaction chromatography with FLD (HPLC-HILIC-FLD) (Fig.1 B), with MS and tandem MS
174 (MS/MS) (Fig.1 C) and matrix assisted laser desorption ionization time-of-flight (MALDI-ToF) MS

(Fig.1 D,E). Initially, this methodology was optimized using commercially available manno- and xylooligosaccharides (X/M 1-6). The products generated at this initial stage were used as standards going forward (Fig.S1). The study also extended to a number of other monomers, oligo- and polysaccharides, observing that this approach is applicable to a wide range of glycans with reducing ends. Retaining structural motifs and decorations, such as, in this case acetylation's, was seen as an essential attribute for the methodology. In the characterisation procedure we observed no appreciable losses of acetylation's in the labelled substrates produced as observed in Fig 1 D.

Substrate purification & Excess label removal. The purification process is of particular importance in this methodology. Numerous studies have reported on the post-labelling purification of 2-AB glycoconjugates, with varying degrees of both success and expense. After trialling numerous solvent and solid phase extraction (SPE) systems (details in supplementary information), our method of choice for substrate purification and excess label removal was liquid-liquid extraction with ethyl acetate. This approach provided clean, almost excess label-free extracts which could be efficiently recovered by drying *in vacuo*. Ethyl acetate was subsequently employed for the extraction of free label in solution, whilst not as efficient as octanal it provided an effective reduction of excess label (Fig. S2).

These experiments were initially carried out on milligram scale and subsequently scaled up (Fig. S3) to produce multi-gram labelled material, therefore enabling this experimental methodology to be efficiently scaled up for bioreactor applications and potential *in vivo* studies.

Fermentations & Growth. To understand both bacterial growth conditions and the optimum conditions for label uptake, the inclusion of labelled substrates to bacterial cultures was performed in one of four ways (Fig. 2). Condition set **2**, consisting in a mixture of glucose and labelled substrate, was chosen going forwards as it provided the best resolution for flow cytometry measurements, as poor or in some instances, no growth on labelled and/or unlabelled substrates (conditions **1**, **3** and **4**) resulted in a lack of viable cells to analyse.

T0 Sampling. Metabolism of labelled carbohydrates was followed by incremental analysis of the isolated supernatant by HPLC-HILIC-FLD. Supernatant product profiles were compared to both standards and negative control samples. Negative controls assigned as T0 samples, consisted of substrates dissolved in fermentation media. True 'T0' samples i.e. samples acquired directly after inoculation of fermentations with labelled substrate, were deemed unfeasible to be used for comparative studies, this was due to rapid carbohydrate degradation and label uptake, even within the relatively short time period of exposure during sampling.

Flow Cytometry. Evaluation of uptake and incorporation of labelled components by bacterial cells isolated from fermentation experiments by flow cytometry led to a clear and distinct identification of labelled cells. A marked shift in fluorescence demonstrated by the implemented gating strategy (355 nm Height vs. 488-FSC2 Height), conclusively confirmed the presence of 2-AB (Fig.3 A-D). The gating strategy incorporated a DNA dye (see *Confocal Microscopy* in the materials and methods section) to ensure only cells were included in the overall identification. Visualisation of the shift in fluorescence and therefore increase in labelled glycan uptake could be more easily displayed and therefore tracked using the plot of 355 nm outlined in Fig. 3E. It should be noted that in numerous experiments rapid uptake was readily

observed, generally though the method could be used effectively to monitor the uptake of labelled glycans in bacterial cells over time.

HPLC-HILIC-FLD. Uptake and utilisation of labelled substrates could be effectively monitored over time by analysis of supernatant sub-samples taken from ongoing anaerobic fermentations (Fig 4). Supernatant samples were compared directly with the labelled starting material added in the initial stages of the fermentation. The substrate used for comparison was also subjected to the same conditions applied in fermentations (Fig 4), thus confirming that any observable degradation occurred as a direct result of bacterial processing of the carbohydrates and not due natural degradation over time from exposure to the controlled anaerobic environment.

A combination of synthetically prepared standards (Fig. S1) and, when required, MALDI-ToF, were applied to characterise the degradation products present in supernatant chromatograms. In either single strain or co-cultured fermentations, the degradation of substrates, observed by the shift of oligosaccharide DP from high to low, was clearly demonstrated through chromatographic and mass spectrometry techniques.

The overall technique developed in this study is demonstrated in Fig. 5, using a single strain (*B. cellulosilyticus*) and a single 2-AB labelled carbohydrate substrate, GH-10-AGX. The bacterial strain grown on the labelled substrate could be effectively monitored over time. Flow cytometry (Fig. 5 A-B) was able to display, through an increase in fluorescent response over time, the higher incorporation levels of the labelled substrate within the cells. While chromatographically, through HPLC-HILIC-FLD monitoring could be employed to follow the

238 contents of the supernatant and the increase or decrease in abundance of certain types and
239 chain lengths of labelled carbohydrates over time (Fig. 5 C). This may be utilized in a number of
240 ways, e.g. to obtain high resolution information on microbial substrate preferences.
241 Furthermore, the fluorescent labelling allows for the use of microscopy to obtain further insight
242 into uptake.

243 **Confocal Microscopy.** Isolated and fixed cells recovered from 2-AB labelled fermentations could
244 be positively screened for and further characterised by confocal microscopy (Fig. 6). DAPI (4',6-
245 diamidino-2-phenylindole) is commonly used for the staining of DNA in microscopy techniques.
246 However, 2-AB - Ex 330 Em 420, has an overlapping Ex/Em range - DAPI Ex 358 Em 461. Two
247 alternative dyes were therefore investigated for DNA staining including SYTO 9 and SYBR Green
248 I, along with two potential stains for membrane identification (FM 5-95 and *Bac*Light Red). SYBR
249 and SYTO 9 both performed efficiently in the staining of bacterial DNA and were used
250 interchangeably for both confocal microscopy and flow cytometry. For cell wall/membrane
251 staining *Bac*Light Red provided marginally more efficient coverage and therefore improved
252 resolution when compared to FM 5-95 in microscopy applications.

253 **Epifluorescence Microscopy.** Alongside confocal microscopy labelled bacterial cells were
254 additionally identified by standard epifluorescence microscopy. The dedicated wavelength for
255 DAPI excitation was used in order to stimulate and view the internalised 2-AB label. Bacterial
256 cells cultured on either mannan or xylan based substrates were clearly identifiable in samples
257 after only 1 hour (Fig. 7). In order to visualize non-labelled cells, the bright field application was
258 utilised to demonstrate the lack of fluorescence in cells grown without 2-AB labelled substrates.

Identification of labelled bacteria through epifluorescence could be routinely employed as a comparatively quick and efficient methodology for labelled-substrate growth confirmation.

A Technique for Screening Microbial Communities/Substrate Specificity. The labelling methodology was further explored through the use of complex glycans. *B. ovatus* (after 24 & 72 hrs) demonstrated incorporation of labelled substrates to differing degrees (Fig. 8). More complex glycans, like AcGGM and AcAGX, both observed the highest uptake levels whilst GH10-AGX and GH26-AcGGM showed much lower levels of incorporation (Fig. 8 B, D). Expanding the experiment focus out to include a range of *Bacteroides* strains, co-cultured with *B. ovatus*, this trend was also widely observed (Fig. 8). However, while chromatographic and MS data generally corresponded well with the accompanying trends identified by the flow numbers, in some cases, despite low inclusion levels observed in the flow, greater levels of glycan degradation was observed when studied by MALDI-ToF and HPLC-HILIC-FLD (Fig. S4 A-B).

The concept of co-culturing bacteria investigating the effect of substrate complexity was further analysed by using a single substrate, AcAGX, to explore the uptake and metabolism in both single and co-cultured bacterial systems (Fig. S5).

Further advancement of labelling capabilities may be achieved by employing both chemical and enzymatic techniques to enhance and expand glycoconjugates for potential microbial consortia analysis(67) (68). Recent studies have indicated that increased consideration is required when selecting substrates to study microbial interactions(69)(70). Studying substrate specificity through a labelling-based approach could help bring a heightened level of knowledge to this area of research. Including other types of labels, specifically a fluorescein-based label such as

FITC as well as 2-AB could help to shed light on the way in which glycans are internalized and degraded as part of a bacterial consortia's catabolism process. Having a wider variety of glycan label alternatives (large, small, flexible, charged) may also help to understand and/or reduce any possible bias that the incorporation of a label may induce. Potential bias could also be addressed by the systematic addition of labels in different positions (on glycans). The addition of labels at either end would further the currently limited studies into the potential directionality(68) of glycan uptake by microbiota. Direct molecular imaging of glycans could be seen as a logical next step and complementary technique to labelling-based approaches(71).

High throughput screening of large numbers of substrates with vast numbers of different microorganisms could be achieved through an integrated plate-based process, linked to a dedicated database system(72), ultimately towards an automated glycomic platform(73). Metagenomics and metaproteomics approaches, in combination with growth and biochemical analysis to assess complex polysaccharide degradation(42), is seen as a key next step for furthering this technique. Additionally heading towards an automated process for identifying specific sub groups of microbial groupings within complex communities, with the idea that such a process could be integrated into a fully rounded 'omics approach(74).

Incorporating cell sorting, coupled with qPCR analysis to enable the continued exploration into understanding glycan metabolism on a genomic level will be further explored. It is envisaged that this technique as a whole could be utilized for selective sorting and identification of microbial communities in relation to microbes' glycan selectivity.

Our combination of techniques and compatible methodologies, implementing a small fluorescent label such as 2-AB (approximately the size of a monosaccharide) for the monitoring and study of glycan uptake allows for the continued development into the high-resolution analysis of microbial systems. In demonstrating this scalable, non-toxic, process of fluorescent coupling, applicable to several types of mono-, oligo- and polysaccharides which include prominent structural features such as acetylations, we have provided a framework for the screening of naturally existing substrates by several complementary techniques. The addition of a fluorophore should help to reduce the number of targets when analyzing large microbial consortia, allowing for a simpler analysis of microbiota compositions, therefore leading to a higher level of precision than is commonly achieved with conventional methodologies.

MATERIALS AND METHODS

Substrates. Mannobiose, mannotriose, mannotetraose, mannopentaose and mannohexaose, xylobiose, xylotriose, xylotetraose, xylopentaose and xylohexaose were from Megazyme (Ireland). Mannose, xylose, 2-picoline borane, 2-aminobenzamide, ethyl acetate, methanol and ammonium formate were purchased from Sigma-Aldrich (Germany).

Acetylated galactoglucomannan (AcGGM) from Norway spruce (*Picea abies*) was produced in house from dried wood chips(75). A simplified (lower DP range) version of this substrate, named GH26-AcGGM was produced by treating the AcGGM with a β-mannanase (*R. intestinalis* β-mannanase *Ri*GH26).

Acetylated (arabino)glucuronoxylan (AcAGX) was produced in house from birch (*Betula pubescens*) chips(76). A simplified (lower DP range and deacetylated) version of this substrate, named GH10-AGX was produced by treating the AcAGX with sodium hydroxide to remove all acetylations followed by subsequent treatment with the commercial xylanase Shearzyme (Novozymes, Denmark).

Procedure for 2-AB Labelling of Mono- & Oligosaccharides as Standards. Reductive amination-based labelling of both mono- and oligosaccharides with 2-AB was loosely based on the original methodology devised by Bigge *et al* 1995(62). However, in this method DMSO was replaced by aqueous acidified methanol and $NaBH_3CN$ with Pic-BH_3 as reported by Vanina *et al* 2011(65).

Small Scale Samples for Standards. In an Eppendorf tube Mannotriose (0.5 mg, 1 umol, 1 equivalent) was dissolved in an amount of H_2O to which a freshly prepared aliquot of Pic-BH_3 (0.52 mg, 5 umol, 5 eq) in methanol was added. To this solution an amount of 2-AB (0.16 mg, 1.1 umol, 1.1 eq) in methanol was added along with a volume of acetic acid to achieve a final solution ratio of 35:50:15 methanol, water, acetic acid respectively (v/v/v). The tube was heated at 60°C for 2 hours and constantly shaken at 500 rpm. After 2 hours the solution was cooled and evaporated to dryness via CentriVap (Labconco, USA). Samples were then reconstituted in water and extracted 3 times with ethyl acetate to remove excess labelling reagent. Samples were then freeze-dried and stored as solids, with tubes wrapped in foil to prevent light degradation.

Gram Scale Preparation of Samples for Fermentation usage. In a 50 mL Falcon tube Mannan/Xylan based polysaccharides (1 g, 1 eq) was dissolved in an amount of H_2O to which a

freshly prepared aliquot of Pic-BH_3 (0.42 g, 5 eq) in methanol was added. To this solution an amount of 2-AB (0.55 g, 5eq) in methanol was added along with a volume of acetic acid to achieve a final solution ratio of 35:50:15 methanol, water, acetic acid respectively (v/v/v). The tube was heated at 60°C for 2 hours in a water bath and constantly agitated. After 2 hours the solution was cooled and evaporated to dryness via CentriVap (Labconco, USA). Samples were then reconstituted in water and extracted 3 times with ethyl acetate to remove excess labelling reagent. Samples were then freeze-dried and stored as solids, with tubes wrapped in foil to prevent light degradation.

Multi-gram Scale Preparation of Samples for Fermentation usage. In a 2 L round bottom flask Mannan/Xylan based polysaccharides (12 g, 1 eq) was dissolved in an amount of H_2O to which a freshly prepared aliquot of Pic-BH_3 (5 g, 5 eq) in methanol was added. To this solution an amount of 2-AB (6.6 g, 5eq) in methanol was added along with a volume of acetic acid to achieve a final solution ratio of 35:50:15 methanol, water, acetic acid respectively (v/v/v). The flask was heated in an oil bath at 60°C for 2 hours in a water bath with constantly stirring. After 2 hours the solution was cooled, and methanol removed by rotary evaporation. Samples were then extracted 3 times with ethyl acetate to remove excess labelling reagent. Residual ethyl acetate was removed by rotary evaporation. The solution was transferred to 50 mL Falcon tubes and freeze-dried. The resulting solids were wrapped in foil to prevent light degradation.

Confocal Methodology. Fluorescently labelled cells were prepared for visualization by adding 1 uL of the fixed cell solution and diluting with 999 uL Pbs, then subsequently stained with 1 uL SYTO 9 (for DNA) and 1 uL *Bac*Light Red (for cell wall) Bacterial Stain Ex581/Em644 (Invitrogen, Thermo Fisher, UK). For mounting, 2 uL of the resulting solution was then added to a poly-D-

363 lysine-coated slide and dried. Slides were then washed with MQ water to remove excess salts
364 and dried again. One drop of Fluoroshield mounting medium (Sigma Aldrich, UK) was then
365 added to the cells followed by the addition of a cover slip. The cells were visualized on a Zeiss
366 LSM 800 confocal laser scanning microscope (Carl Zeiss, Germany) using the following nm lasers
367 - 561 (558-575) for cell wall, 488 (483-500) for DNA and 405 (353-465) for 2-AB. All images were
368 processed using the Zen Blue Edition software v.3.0 (Carl Zeiss, Germany).

369 **Epifluorescence Methodology.** In addition to confocal microscopy, cells were also viewed and
370 identified as fluorescently labelled by epifluorescence microscopy. Labelled bacterial cells (0.4
371 µL) were mounted onto agarose-coated (1.2%) glass slides and secured with coverslips.
372 Unlabelled cells were also treated in the same way. Visualization was achieved using the DAPI
373 wavelength (1.5 second exposure time) whilst negative control samples were also viewed using
374 the brightfield to add further confirmation. Cells were observed on a Zeiss microscope (Carl
375 Zeiss, Germany) – Axio Observer Z1/LSM700 – HXP-120 Illuminator (fluorescence light source).
376 Images were acquired using an ORCA-Flash4.0 V2 Digital CMOS camera (Hamamatsu Photonics)
377 through a 100x phase-contrast objective. All images were analyzed with the Zen Blue Edition
378 software v.3.0 (Carl Zeiss, Germany).

379 **Fermentations.** Human-gut derived *Bacteroides* sp. (*B. thetaiotamicron* 7330(77), *B. ovatus*
380 ATCC 8483(77), *B. cellulosyliticus* DSM 14838(78) and *B. caccae* ATCC 43185(79)) were cultured
381 into freshly prepared minimal medium (MM)(80) supplemented with 5 mg/mL glucose. All
382 fermentations were performed at 37°C in an anaerobic cabinet (Whitley A95 Workstation; Don
383 Whitley, UK) under an 85% N_2, 5% CO_2 and 10% H_2 atmosphere. Where fermentations were
384 supplemented with labelled substrates, an aliquot of an initial overnight fermentation (as

previously described) was taken and inoculated into a solution containing freshly made 2X MM (50% v) along with an amount of labelled substrate and equivalent glucose solution (50% v). Co-cultured samples were initially grown independently as described above; overnight samples were then combined into freshly prepared MM with 5 mg/mL glucose and grown overnight before the introduction of labelled substrates as described above.

Fermentation Sampling. Samples taken from fermentations were processed immediately to minimize any changes to cell dynamics/conditions. 100 uL samples were recovered at each specified time point and transferred to Eppendorf tubes. Samples were then centrifuged (14,000 rpm, 4 minutes), after which the supernatant was frozen and stored at -20°C for further analysis. The cells were then fixed by resuspending the cell pellet in 100 uL 2% paraformaldehyde (PFA) - 4% solution diluted in Pbs (Invitrogen, Thermo Fisher, UK) for 1 hour at room temperature. After 1 hour samples were centrifuged (14,000 rpm, 4 minutes) and the supernatant discarded. The pellet was then washed with Phosphate-buffered saline (PBS; pH 7.4 – 137 mM NaCl, 2.7 mM KCl, 10 mM Na_2HPO_4, 1.8 mM KH_2PO_4) – vortex, centrifuge, discard supernatant. Finally, the pellet was resuspended in PBS and stored at 4°C for further analysis.

Flow Cytometry Analysis. Samples used for flow cytometry analysis were thawed on ice and appropriately diluted in PBS – commonly 1/500, to achieve optimal cell density for flow. Samples were stained for DNA using either SYBR Green I Nucleic acid gel stain Ex504/Em523 (10,000 X concentrate in DMSO – subsequently diluted to 1:1000) (Invitrogen, Thermo Fisher, UK) or SYTO 9 Green Fluorescent Nucleic acid stain Ex485/Em498, diluted 1:1000 (Invitrogen, Thermo Fisher, UK). Sample solutions were flowed on a Beckman Coulter Moflo Astrios Eq, typically collecting 50-100,000 events per sample (minimum of 10,000 was used when analyzing

fermentations demonstrating minimal growth) and at a constant flow rate (slow). All data was processed using the Kaluza analysis software v.2.1. Firstly, for each bacterial species a "negative" sample (24 hours growth on unlabelled substrate) was flowed in order to establish a gating protocol as to only process events/cells which were positive for SYBR/SYTO DNA staining (488-FSC2 Height predominantly used). Samples were then deemed to be "fluorescently labelled" or not by a positive shift in the correlation of 488-FSC2 Height vs. 355-448/59 Height (fluorescence intensity threshold).

HPLC Supernatant Analysis. For the analysis of 2-AB labelled standards as well as recovered fermentation supernatants hydrophilic interaction chromatography (HILIC), was applied using an Agilent 1290 Infinity (Agilent Technologies, Santa Clara, CA, USA) UHPLC system. The methodology was based on that developed by Westereng *et al* 2020(68), with the following modifications. The system was connected in parallel (1:10 split) to an Agilent 1260 fluorescence detector – Ex 330 nm, Em 420 nm (Agilent Technologies, Santa Clara, CA, USA) and a Velos pro LTQ linear ion trap (Thermo Scientific, San Jose, CA, USA). The HILIC column (bioZen Glycan, 2.6 µm, 2.1 x 100 mm) including a guard column (SecurityGuard ULTRA with bioZen Glycan cartridge, 2.1 x 2 mm) was operated at 50 °C, running at 0.3 mL/min, and using 50 mM ammonium formate pH 4.4 (eluent A) and 100 % acetonitrile (eluent B). Samples were eluted using the following gradient: initial starting ratio of 90 % B and 10 % A, gradient to 72 % B and 28 % A from 0 to 16 mins, gradient to 40 % B and 60 % A from 16 to 20 mins, isocratic from 20 to 25 mins, gradient to 76 % B and 24 % A from 25 to 27 mins, isocratic from 27 to 30 mins . Two µL of the samples were injected.

HPLC-HILIC-FLD (MS) of Substrates. For HILIC-FLD-MS the instrument was operated in positive mode with an ionization voltage of 3.5 kV, auxiliary and sheath gas settings of 5 and 30 respectively (arbitrary units) and with capillary and source temperatures of 300 °C and 250 °C, respectively. The scan range was set to *m/z* 110–2000 and MS/MS analysis was performed with CID fragmentation with helium as the collision gas. All data were recorded with Xcalibur version 2.2.

MALDI-ToF. MALDI-ToF analyses were conducted using an Ultraflex MALDI-ToF/ToF instrument (Bruker Daltonics, Germany) equipped with a 337-nm-wavelength nitrogen laser. All measurements were performed in positive mode. Data were collected from 100 laser shots using the lowest energy level necessary to obtain sufficient spectral intensity. The mass spectrometer was calibrated with a mixture of manno-oligosaccharides or xylo-oligosaccharides (DP, 2 to 6) obtained from Megazyme. For sample preparation, 1 µL of sample solution was mixed with 2 µL of matrix (9 mg/mL 2,5-dihydroxybenzoic acid (DHB)–30% acetonitrile v/v), directly applied on a MTP 384 target plate (Bruker Daltonics, Germany), and dried under a stream of warm air.

Data availability. All data supporting the findings of this study are available within the article and supplemental material.

SUPPLEMENTAL MATERIAL

Supplemental material is available online only.

Fig. S1, Word file, 0.24 MB

448 **Fig. S2**, Word file, 0.15 MB

449 **Fig. S3**, Word file, 0.16 MB

450 **Fig. S4**, Word file, 0.32 MB

451 **Fig. S5**, Word file, 0.33 MB

452 **ACKNOWLEDGMENTS**

453 We are grateful for support from The Research Council of Norway (BIONÆR program to B.W.:
454 244259).

455 S.L and L.L. performed flow cytometry and confocal microscopy. S.L. carried out all other
456 analysis. S.L. and B.W. conceived the study and supervised the research. The manuscript was
457 primarily written by S.L. with contributions from B.W., S.L.L.R. and L.L. Figures were prepared
458 by S.L.

459 We declare that we have no competing interests.

460

461 **REFERENCES**

462 1. Kaoutari A El, Armougom F, Gordon JI, Raoult D, Henrissat B. 2013. The abundance and
463 variety of carbohydrate-active enzymes in the human gut microbiota. Nat Rev Microbiol
464 11:497–504.

465 2. La Rosa SL, Kachrimanidou V, Buffetto F, Pope PB, Pudlo NA, Martens EC, Rastall RA,
466 Gibson GR, Westereng B. 2019. Wood-Derived Dietary Fibers Promote Beneficial Human

Gut Microbiota. mSphere 4.

3. Xu J, Chiang HC, Bjursell MK, Gordon JI. 2004. Message from a human gut symbiont: Sensitivity is a prerequisite for sharing. Trends Microbiol. Elsevier Ltd.

4. Briggs JA, Grondin JM, Brumer H. 2020. Communal living: glycan utilization by the human gut microbiota. Environ Microbiol 1462-2920.15317.

5. Abou Hachem M, Andersen JM, Barrangou R, Moller MS, Fredslund F, Majumder A, Ejby M, Lahtinen SJ, Jacobsen S, Lo Leggio L, Goh YJ, Klaenhammer TR, Svensson B. 2013. Recent insight into oligosaccharide uptake and metabolism in probiotic bacteria. Biocatal Biotransformation. Taylor & Francis.

6. Theilmann MC, Goh YJ, Nielsen KF, Klaenhammer TR, Barrangou R, Hachem MA. 2017. Lactobacillus acidophilus metabolizes dietary plant glucosides and externalizes their bioactive phytochemicals. MBio 8.

7. Savage DC. 1977. Microbial ecology of the gastrointestinal tract. Annu Rev Microbiol. Annual Reviews 4139 El Camino Way, P.O. Box 10139, Palo Alto, CA 94303-0139, USA .

8. Trastoy B, Du JJ, Klontz EH, Li C, Cifuente JO, Wang LX, Sundberg EJ, Guerin ME. 2020. Structural basis of mammalian high-mannose N-glycan processing by human gut Bacteroides. Nat Commun 11.

9. Glowacki RWP, Martens EC. 2020. If you eat it, or secrete it, they will grow: the expanding list of nutrients utilized by human gut bacteria. J Bacteriol https://doi.org/10.1128/jb.00481-20.

487 10. Sanders ME, Merenstein DJ, Reid G, Gibson GR, Rastall RA. 2019. Probiotics and
488 prebiotics in intestinal health and disease: from biology to the clinic. Nat Rev
489 Gastroenterol Hepatol. Nature Publishing Group.

490 11. Gibson GR, Hutkins R, Ellen Sanders M, Prescott SL, Reimer RA, Salminen SJ, Scott K,
491 Stanton C, Swanson KS, Cani PD, Verbeke K, Reid G. 2017. Expert consensus document:
492 The International Scientific Association for Probiotics and Prebiotics (ISAPP) consensus
493 statement on the definition and scope of prebiotics. Nat Publ Gr 14.

494 12. Lombard V, Golaconda Ramulu H, Drula E, Coutinho PM, Henrissat B. 2014. The
495 carbohydrate-active enzymes database (CAZy) in 2013. Nucleic Acids Res 42:D490–D495.

496 13. Xu J, Bjursell MK, Himrod J, Deng S, Carmichael LK, Chiang HC, Hooper L V., Gordon JI.
497 2003. A genomic view of the human-Bacteroides thetaiotaomicron symbiosis. Science
498 (80-) 299:2074–2076.

499 14. Bjursell MK, Martens EC, Gordon JI. 2006. Functional genomic and metabolic studies of
500 the adaptations of a prominent adult human gut symbiont, Bacteroides
501 thetaiotaomicron, to the suckling period. J Biol Chem 281:36269–36279.

502 15. Déjean G, Tamura K, Cabrera A, Jain N, Pudlo NA, Pereira G, Viborg AH, Van Petegem F,
503 Martens EC, Brumer H. 2020. Synergy between cell surface glycosidases and glycan-
504 binding proteins dictates the utilization of specific beta(1,3)- glucans by human Gut
505 Bacteroides. MBio 11.

506 16. Martens EC, Koropatkin NM, Smith TJ, Gordon JI. 2009. Complex glycan catabolism by

the human gut microbiota: The bacteroidetes sus-like paradigm. J Biol Chem. Elsevier.

17. Anderson KL, Salyers AA. 1989. Biochemical evidence that starch breakdown by Bacteroides thetaiotaomicron involves outer membrane starch-binding sites and periplasmic starch-degrading enzymes. J Bacteriol 171:3192–3198.

18. Glenwright AJ, Pothula KR, Bhamidimarri SP, Chorev DS, Baslé A, Firbank SJ, Zheng H, Robinson C V., Winterhalter M, Kleinekathöfer U, Bolam DN, Van Den Berg B. 2017. Structural basis for nutrient acquisition by dominant members of the human gut microbiota. Nature 541:407–411.

19. Gray DA, White JBR, Oluwole AO, Rath P, Glenwright AJ, Mazur A, Zahn M, Baslé A, Morland C, Evans SL, Cartmell A, Robinson C V., Hiller S, Ranson NA, Bolam DN, van den Berg B. 2021. Insights into SusCD-mediated glycan import by a prominent gut symbiont. Nat Commun 12:1–14.

20. Madej M, White JBR, Nowakowska Z, Rawson S, Scavenius C, Enghild JJ, Bereta GP, Pothula K, Kleinekathoefer U, Baslé A, Ranson NA, Potempa J, van den Berg B. 2020. Structural and functional insights into oligopeptide acquisition by the RagAB transporter from Porphyromonas gingivalis. Nat Microbiol 5:1016–1025.

21. Leth ML, Ejby M, Workman C, Ewald DA, Pedersen SS, Sternberg C, Bahl MI, Licht TR, Aachmann FL, Westereng B, Hachem MA. 2018. Differential bacterial capture and transport preferences facilitate co-growth on dietary xylan in the human gut. Nat Microbiol 3:570–580.

527 22. La Rosa SL, Leth ML, Michalak L, Hansen ME, Pudlo NA, Glowacki R, Pereira G, Workman
528 CT, Arntzen M, Pope PB, Martens EC, Hachem MA, Westereng B. 2019. The human gut
529 Firmicute Roseburia intestinalis is a primary degrader of dietary β-mannans. Nat
530 Commun 10.

531 23. Lindstad LJ, Lo G, Leivers S, Lu Z, Michalak L, Pereira V, Røhr ÅK, Martens EC, McKee LS,
532 Westereng B, Pope PB, Leanti La Rosa S. 2020. Human gut Faecalibacterium prausnitzii
533 deploy a highly efficient conserved 1 system to cross-feed on β-mannan-derived
534 oligosaccharides 2 Running title: β-MOS depolymerization by Faecalibacterium
535 prausnitzii. bioRxiv 2020.12.23.424282.

536 24. Crouch LI, Liberato M V., Urbanowicz PA, Baslé A, Lamb CA, Stewart CJ, Cooke K, Doona
537 M, Needham S, Brady RR, Berrington JE, Madunic K, Wuhrer M, Chater P, Pearson JP,
538 Glowacki R, Martens EC, Zhang F, Linhardt RJ, Spencer DIR, Bolam DN. 2020. Prominent
539 members of the human gut microbiota express endo-acting O-glycanases to initiate
540 mucin breakdown. Nat Commun 11:1–13.

541 25. Briliūtė J, Urbanowicz PA, Luis AS, Baslé A, Paterson N, Rebello O, Hendel J, Ndeh DA,
542 Lowe EC, Martens EC, Spencer DIR, Bolam DN, Crouch LI. 2019. Complex N-glycan
543 breakdown by gut Bacteroides involves an extensive enzymatic apparatus encoded by
544 multiple co-regulated genetic loci. Nat Microbiol 4:1571–1581.

545 26. Michalak L, Gaby JC, Lagos L, La Rosa SL, Hvidsten TR, Tétard-Jones C, Willats WGT,
546 Terrapon N, Lombard V, Henrissat B, Dröge J, Arntzen MØ, Hagen LH, Øverland M, Pope
547 PB, Westereng B. 2020. Microbiota-directed fibre activates both targeted and secondary

548 metabolic shifts in the distal gut. Nat Commun 11:1–15.

549 27. Patnode ML, Beller ZW, Han ND, Cheng J, Peters SL, Terrapon N, Henrissat B, Le Gall S,
550 Saulnier L, Hayashi DK, Meynier A, Vinoy S, Giannone RJ, Hettich RL, Gordon JI. 2019.
551 Interspecies Competition Impacts Targeted Manipulation of Human Gut Bacteria by
552 Fiber-Derived Glycans. Cell 179:59-73.e13.

553 28. La Rosa SL, Leth ML, Michalak L, Hansen ME, Pudlo NA, Glowacki R, Pereira G, Workman
554 CT, Arntzen M, Pope PB, Martens EC, Hachem MA, Westereng B. 2019. The human gut
555 Firmicute Roseburia intestinalis is a primary degrader of dietary β-mannans. Nat
556 Commun 10:1–14.

557 29. Geva-Zatorsky N, Alvarez D, Hudak JE, Reading NC, Erturk-Hasdemir D, Dasgupta S, Von
558 Andrian UH, Kasper DL. 2015. In vivo imaging and tracking of host-microbiota
559 interactions via metabolic labeling of gut anaerobic bacteria. Nat Med 21:1091–1100.

560 30. Hehemann JH, Reintjes G, Klassen L, Smith AD, Ndeh D, Arnosti C, Amann R, Abbott DW.
561 2019. Single cell fluorescence imaging of glycan uptake by intestinal bacteria. ISME J
562 13:1883–1889.

563 31. Reintjes G, Arnosti C, Fuchs BM, Amann R. 2017. An alternative polysaccharide uptake
564 mechanism of marine bacteria. ISME J 11:1640–1650.

565 32. McNulty NP, Wu M, Erickson AR, Pan C, Erickson BK, Martens EC, Pudlo NA, Muegge BD,
566 Henrissat B, Hettich RL, Gordon JI. 2013. Effects of Diet on Resource Utilization by a
567 Model Human Gut Microbiota Containing Bacteroides cellulosilyticus WH2, a Symbiont

568 with an Extensive Glycobiome. PLoS Biol 11.

569 33. Deehan EC, Yang C, Perez-Muñoz ME, Nguyen NK, Cheng CC, Triador L, Zhang Z, Bakal JA,
570 Walter J. 2020. Precision Microbiome Modulation with Discrete Dietary Fiber Structures
571 Directs Short-Chain Fatty Acid Production. Cell Host Microbe 27:389-404.e6.

572 34. Flint HJ, Scott KP, Duncan SH, Louis P, Forano E. 2012. Microbial degradation of complex
573 carbohydrates in the gut. Gut Microbes. Taylor & Francis.

574 35. Ndeh D, Gilbert HJ. 2018. Biochemistry of complex glycan depolymerisation by the
575 human gut microbiota. FEMS Microbiol Rev 002:146–164.

576 36. Flint HJ, Bayer EA, Rincon MT, Lamed R, White BA. 2008. Polysaccharide utilization by gut
577 bacteria: Potential for new insights from genomic analysis. Nat Rev Microbiol.

578 37. Klassen L, Reintjes G, Tingley JP, Jones DR, Hehemann J-H, Smith AD, Schwinghamer TD,
579 Arnosti C, Jin L, Alexander TW, Amundsen C, Thomas D, Amann R, McAllister TA, Abbott
580 DW. 2021. Quantifying fluorescent glycan uptake to elucidate strain-level variability in
581 foraging behaviors of rumen bacteria. Microbiome 9:23.

582 38. Boulos S, Nyström L. 2017. Complementary Sample Preparation Strategies for Analysis of
583 Cereal β-Glucan Oxidation Products by UPLC-MS/MS. Front Chem 5:90.

584 39. Urbanowicz BR, Peña MJ, Moniz HA, Moremen KW, York WS. 2014. Two Arabidopsis
585 proteins synthesize acetylated xylan *in vitro*. Plant J 80:197–206.

586 40. Doud DFR, Bowers RM, Schulz F, De Raad M, Deng K, Tarver A, Glasgow E, Vander
587 Meulen K, Fox B, Deutsch S, Yoshikuni Y, Northen T, Hedlund BP, Singer SW, Ivanova N,

588 Woyke T. 2019. Function-driven single-cell genomics uncovers cellulose-degrading
589 bacteria from the rare biosphere. ISME J https://doi.org/10.1038/s41396-019-0557-y.

590 41. Arnosti C. 2003. Fluorescent derivatization of polysaccharides and carbohydrate-
591 containing biopolymers for measurement of enzyme activities in complex media. J
592 Chromatogr B Anal Technol Biomed Life Sci 793:181–191.

593 42. Unfried F, Becker S, Robb CS, Hehemann JH, Markert S, Heiden SE, Hinzke T, Becher D,
594 Reintjes G, Krüger K, Avcı B, Kappelmann L, Hahnke RL, Fischer T, Harder J, Teeling H,
595 Fuchs B, Barbeyron T, Amann RI, Schweder T. 2018. Adaptive mechanisms that provide
596 competitive advantages to marine bacteroidetes during microalgal blooms. ISME J
597 12:2894–2906.

598 43. Zhang Y, Wang C, Liu Y, Yao W, Sun Y, Zhang P, Huang L, Wang Z. 2014. Fluorescein-5-
599 thiosemicarbazide (FTSC) labeling for fluorescent imaging of pectin-derived
600 oligogalacturonic acid transported in living cells by confocal microscopy. Eur Food Res
601 Technol 239:867–875.

602 44. Thomas B, Yan KC, Hu X Le, Donnier-Maréchal M, Chen GR, He XP, Vidal S. 2020.
603 Fluorescent glycoconjugates and their applications. Chem Soc Rev. Royal Society of
604 Chemistry.

605 45. Pabst M, Kolarich D, Pöltl G, Dalik T, Lubec G, Hofinger A, Altmann F. 2009. Comparison
606 of fluorescent labels for oligosaccharides and introduction of a new postlabeling
607 purification method. Anal Biochem 384:263–273.

608 46. Shilova N V., Bovin N V. 2003. Fluorescent labels for analysis of mono- and
609 oligosaccharides. Bioorg Khim. Springer.

610 47. Harvey DJ. 2011. Derivatization of carbohydrates for analysis by chromatography;
611 electrophoresis and mass spectrometry. J Chromatogr B Anal Technol Biomed Life Sci.
612 Elsevier.

613 48. Achilles J, Stahl F, Harms H, Müller S. 2007. Isolation of intact RNA from cytometrically
614 sorted Saccharomyces cerevisiae for the analysis of intrapopulation diversity of gene
615 expression. Nat Protoc 2:2203–2211.

616 49. Achilles J, Müller S, Bley T, Babel W. 2004. Affinity of single S. cerevisiae cells to 2-
617 NBDglucose under changing substrate concentrations. Cytom Part A 61:88–98.

618 50. Yoshioka K, Saito M, Oh KB, Nemoto Y, Matsuoka H, Natsume M, Abe H. 1996.
619 Intracellular fate of 2-NBDG, a fluorescent probe for glucose uptake activity, in
620 escherichia coli cells. Biosci Biotechnol Biochem 60:1899–1901.

621 51. Tao J, McCourt C, Sultana H, Nelson C, Driver J, Hackmanna TJ. 2019. Use of a fluorescent
622 analog of glucose (2-NBDG) To identify uncultured rumen bacteria that take up glucose.
623 Appl Environ Microbiol 85.

624 52. Ruhaak LR, Zauner G, Huhn C, Bruggink C, Deelder AM, Wuhrer M. 2010. Glycan labeling
625 strategies and their use in identification and quantification. Anal Bioanal Chem. Springer.

626 53. Fang J, Qin G, Ma J, She YM. 2015. Quantification of plant cell wall monosaccharides by
627 reversed-phase liquid chromatography with 2-aminobenzamide pre-column

derivatization and a non-toxic reducing reagent 2-picoline borane. J Chromatogr A 1414:122–128.

54. Vreeker GCM, Wuhrer M. 2017. Reversed-phase separation methods for glycan analysis. Anal Bioanal Chem. Springer Verlag.

55. Melmer M, Stangler T, Premstaller A, Lindner W. 2011. Comparison of hydrophilic-interaction, reversed-phase and porous graphitic carbon chromatography for glycan analysis. J Chromatogr A 1218:118–123.

56. Ahn J, Bones J, Yu YQ, Rudd PM, Gilar M. 2010. Separation of 2-aminobenzamide labeled glycans using hydrophilic interaction chromatography columns packed with 1.7 µm sorbent. J Chromatogr B Anal Technol Biomed Life Sci 878:403–408.

57. Higel F, Demelbauer U, Seidl A, Friess W, Sörgel F. 2013. Reversed-phase liquid-chromatographic mass spectrometric N-glycan analysis of biopharmaceuticals. Anal Bioanal Chem 405:2481–2493.

58. Prater BD, Connelly HM, Qin Q, Cockrill SL. 2009. High-throughput immunoglobulin G N-glycan characterization using rapid resolution reverse-phase chromatography tandem mass spectrometry. Anal Biochem 385:69–79.

59. Lattová E, Snovida S, Perreault H, Krokhin O. 2005. Influence of the labeling group on ionization and fragmentation of carbohydrates in mass spectrometry. J Am Soc Mass Spectrom 16:683–696.

60. Guile GR, Rudd PM, Wing DR, Prime SB, Dwek RA. 1996. A rapid high-resolution high-

performance liquid chromatographic method for separating glycan mixtures and analyzing oligosaccharide profiles. Anal Biochem 240:210–226.

61. Shang TQ, Saati A, Toler KN, Mo J, Li H, Matlosz T, Lin X, Schenk J, Ng C-K, Duffy T, Porter TJ, Rouse JC. 2014. Development and application of a robust N-glycan profiling method for heightened characterization of monoclonal antibodies and related glycoproteins. J Pharm Sci 103:1967–1978.

62. Bigge JC, Patel TP, Bruce JA, Goulding PN, Charles SM, Parekh RB. 1995. Nonselective and efficient fluorescent labeling of glycans using 2-amino benzamide and anthranilic acid. Anal Biochem 230:229–238.

63. Sato S, Sakamoto T, Miyazawa E, Kikugawa Y. 2004. One-pot reductive amination of aldehydes and ketones with α-picoline-borane in methanol, in water, and in neat conditions. Tetrahedron 60:7899–7906.

64. Unterieser I, Mischnick P. 2011. Labeling of oligosaccharides for quantitative mass spectrometry. Carbohydr Res 346:68–75.

65. Cosenza VA, Navarro DA, Stortz CA. 2011. Usage of α-picoline borane for the reductive amination of carbohydrates. Arkivoc 182–194.

66. Ruhaak LR, Steenvoorden E, Koeleman CAM, Deelder AM, Wuhrer M. 2010. 2-Picoline-borane: A non-toxic reducing agent for oligosaccharide labeling by reductive amination. Proteomics 10:2330–2336.

67. Frommhagen M, van Erven G, Sanders M, van Berkel WJH, Kabel MA, Gruppen H. 2017.

668 RP-UHPLC-UV-ESI-MS/MS analysis of LPMO generated C4-oxidized gluco-oligosaccharides
669 after non-reductive labeling with 2-aminobenzamide. Carbohydr Res 448:191–199.

670 68. Westereng B, Kračun SK, Leivers S, Arntzen M, Aachmann FL, Eijsink VGH. 2020. Synthesis
671 of glycoconjugates utilizing the regioselectivity of a lytic polysaccharide monooxygenase.
672 Sci Rep 10:1–15.

673 69. Gray DA, White JBR, Oluwole AO, Rath P, Glenwright AJ, Mazur A, Zahn M, Baslé A,
674 Morland C, Evans SL, Cartmell A, Robinson C V., Hiller S, Ranson NA, Bolam DN, van den
675 Berg B. 2021. Insights into SusCD-mediated glycan import by a prominent gut symbiont.
676 Nat Commun 12:1–14.

677 70. Tamura K, Dejean G, Van Petegem F, Brumer H. 2021. Distinct protein architectures
678 mediate species-specific beta-glucan binding and metabolism in the human gut
679 microbiota. J Biol Chem 296:100415.

680 71. Wu X, Delbianco M, Anggara K, Michnowicz T, Pardo-Vargas A, Bharate P, Sen S, Pristl M,
681 Rauschenbach S, Schlickum U, Abb S, Seeberger PH, Kern K. 2020. Imaging single glycans.
682 Nature 582:375–378.

683 72. Royle L, Campbell MP, Radcliffe CM, White DM, Harvey DJ, Abrahams JL, Kim YG, Henry
684 GW, Shadick NA, Weinblatt ME, Lee DM, Rudd PM, Dwek RA. 2008. HPLC-based analysis
685 of serum N-glycans on a 96-well plate platform with dedicated database software. Anal
686 Biochem 376:1–12.

687 73. Walsh I, O'Flaherty R, Rudd PM. 2017. Bioinformatics applications to aid high-throughput

688 glycan profiling. Perspect Sci 11:31–39.

689 74. Bennke CM, Reintjes G, Schattenhofer M, Ellrott A, Wulf J, Zeder M, Fuchs BM. 2016.
690 Modification of a high-throughput automatic microbial cell enumeration system for
691 shipboard analyses. Appl Environ Microbiol 82:3289–3296.

692 75. Michalak L, Knutsen SH, Aarum I, Westereng B. 2018. Effects of pH on steam explosion
693 extraction of acetylated galactoglucomannan from Norway spruce. Biotechnol Biofuels
694 11:311.

695 76. Dysvik A, La Rosa SL, Buffetto F, Liland KH, Myhrer KS, Rukke EO, Wicklund T, Westereng
696 B. 2020. Secondary Lactic Acid Bacteria Fermentation with Wood-Derived
697 Xylooligosaccharides as a Tool to Expedite Sour Beer Production. J Agric Food Chem
698 68:301–314.

699 77. Wu M, McNulty NP, Rodionov DA, Khoroshkin MS, Griffin NW, Cheng J, Latreille P,
700 Kerstetter RA, Terrapon N, Henrissat B, Osterman AL, Gordon JI. 2015. Genetic
701 determinants of in vivo fitness and diet responsiveness in multiple human gut
702 Bacteroides. Science (80-) 350.

703 78. Robert C, Chassard C, Lawson PA, Bernalier-Donadille A. 2007. Bacteroides cellulosilyticus
704 sp. nov., a cellulolytic bacterium from the human gut microbial community. Int J Syst Evol
705 Microbiol 57:1516–1520.

706 79. Johnson JL, Moore WEC, Moore LVH. 1986. Bacteroides caccae sp. nov., Bacteroides
707 merdae sp. nov., and Bacteroides stercoris sp. nov. isolated from human feces. Int J Syst

Bacteriol 36:499–501.

80. Martens EC, Chiang HC, Gordon JI. 2008. Mucosal Glycan Foraging Enhances Fitness and Transmission of a Saccharolytic Human Gut Bacterial Symbiont. Cell Host Microbe 4:447–457.

FIGURES

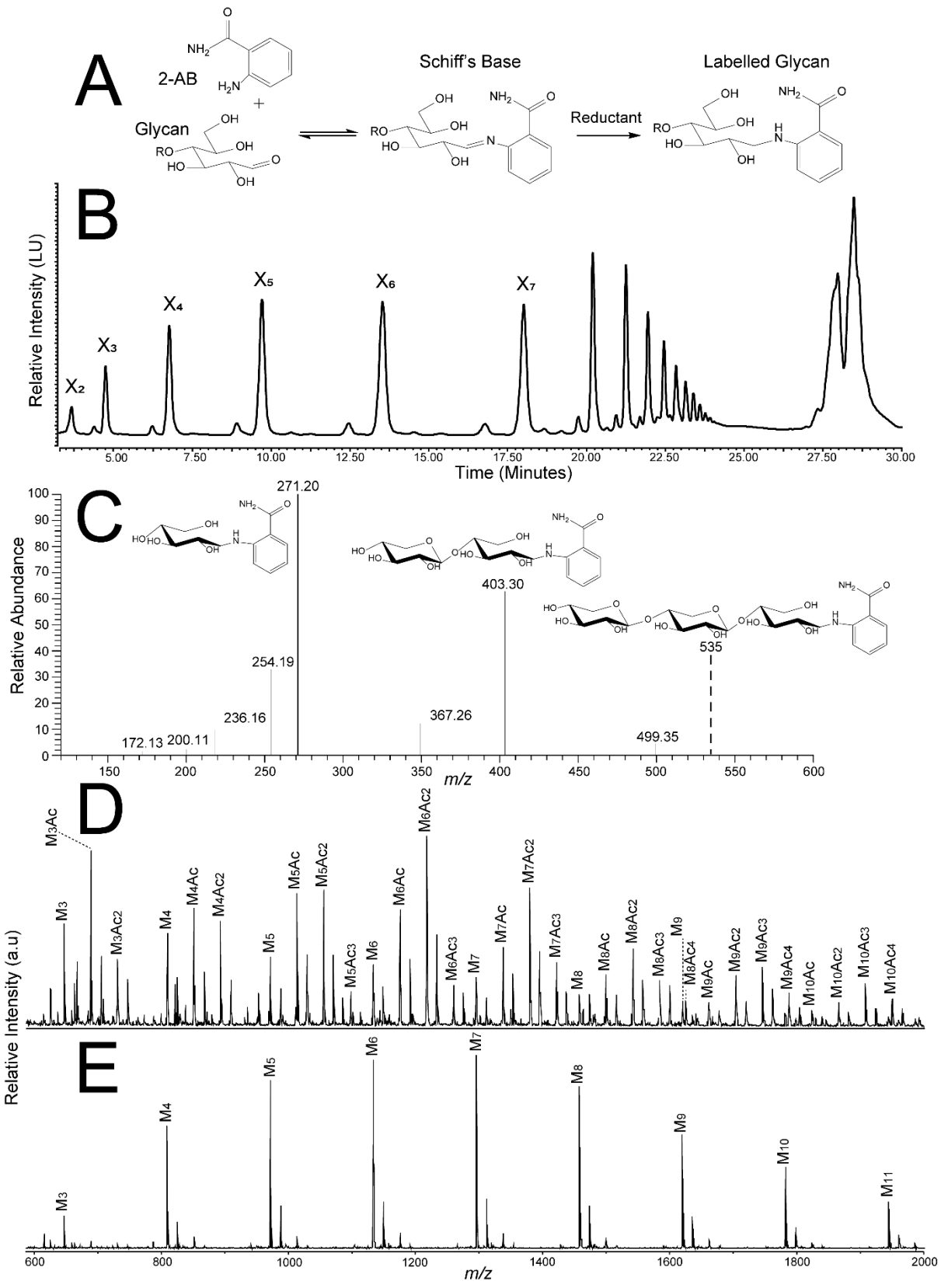

714

Fig.1 – Synthesis and Characterisation of 2-AB Labelled Glycans - **A** – Schematic of synthetic pathway for 2-AB labelling of glycans. **B** – HPLC-HILIC-FLD chromatogram of 2-AB labelled xylan-derived oligosaccharides. **C** – Corresponding MS and MS/MS fragmentation of 2-AB labelled xylotriose – major fragments are 2-AB xylobiose and 2-AB xylose. **D** – MALDI-ToF identification of 2-AB labelled AcGGM – the spectra clearly demonstrates the retention of acetylations after both initial labelling and purification. **E** – MALDI-ToF identification of 2-AB AcGGM (post-labelling deacetylation). In panels B, D, E the following abbreviations are used: X, xylose unit; M, mannose unit, Ac, acetyl group.

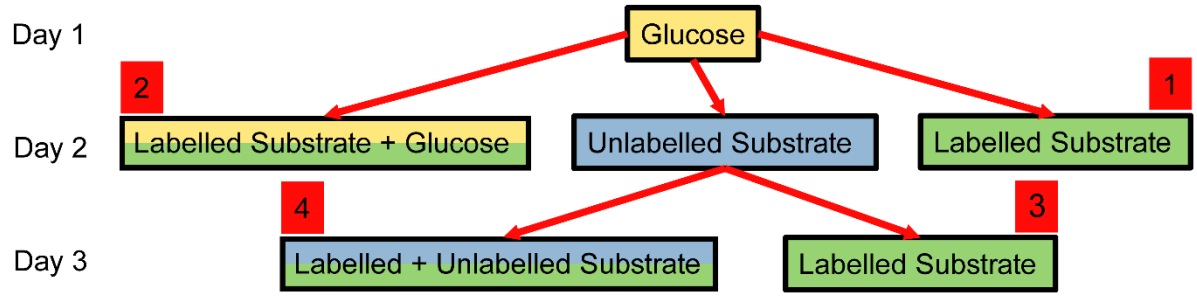

Fig.2 – Plan implemented to determine the most efficient method of identifying labelled glycan uptake. Condition set **1** added to overnight glucose-grown culture, **2** introduced as a mixture of glucose and labelled substrate to overnight glucose-grown culture, **3** overnight glucose-grown culture supplemented with unlabelled substrate, followed by next day addition of either labelled substrate or **4** a mix of labelled & unlabelled substrates. Glucose (yellow), Unlabelled (blue), labelled (green).

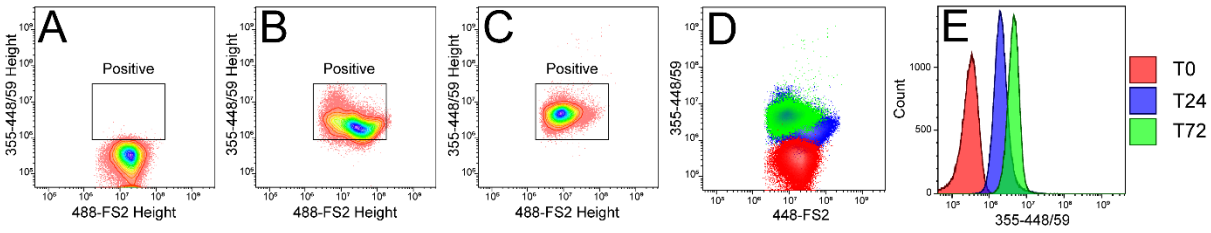

731 Fig.3 – Flow cytometry of *B. cellulosilyticus* grown on AcGGM. **A-D** - Gating strategy developed
732 based on 355 nm Height (2-AB) vs. 488-FSC2 Height (DNA-dye), clearly observed shifts based in
733 fluorescence of bacteria grown on unlabelled glycans **A** T0, compared to bacteria grown on
734 labelled substrates for T 24 **B** or T 72 hr **C**. **D** The overlapped dot-plot demonstrates the
735 incorporation over time by increasing levels of fluorescence (labelled cells. *B. cellulosilyticus*
736 grown on AcGGM) at 24 hr (blue) and 72 hr (green) compared to the unlabelled substrate (red).
737 **E** - Histogram indicating the shift in fluorescence observed for cells grown on labelled
738 substrates for 24 hr (blue) and 72hr (green) compared to the unlabelled substrate (red).

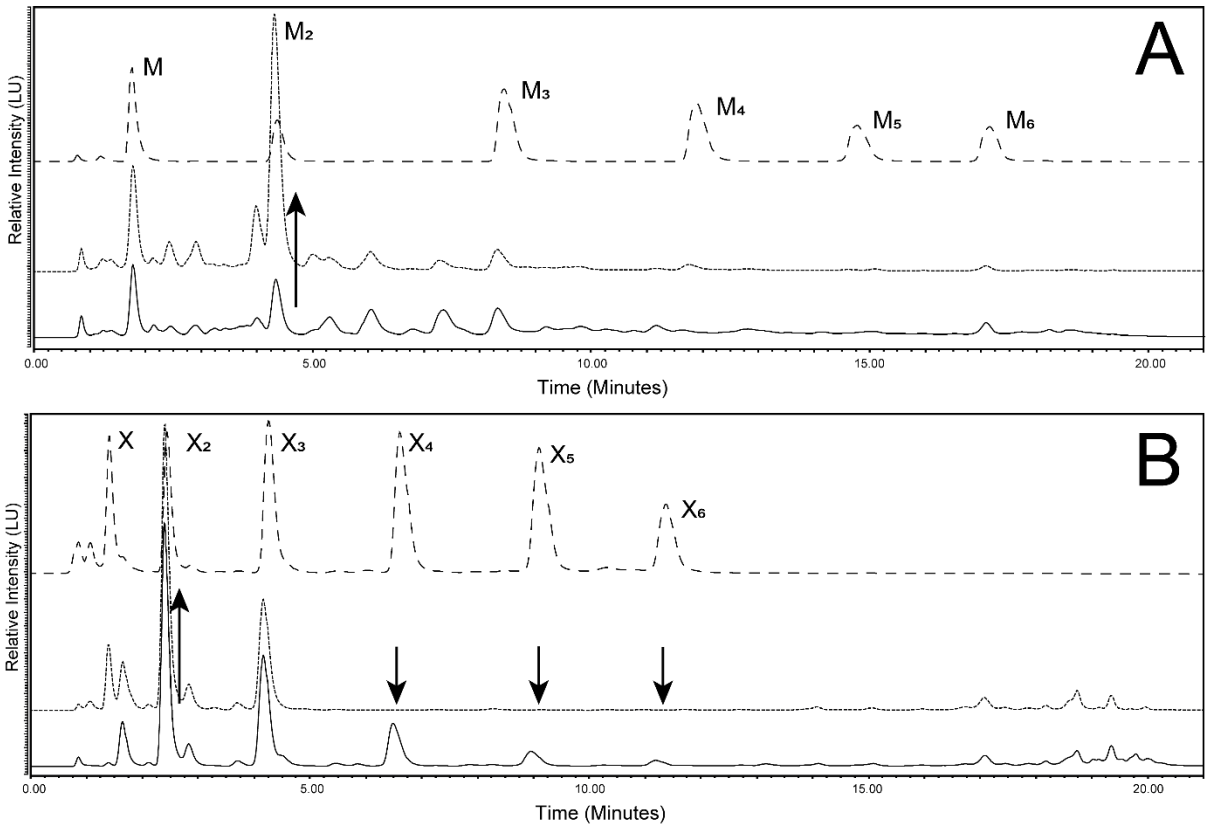

739

740 Fig.4 – Monitoring of fluorescently labelled substrate metabolism by HPLC-HILIC-FLD. **A –** *B.*
741 *cellulosilyticus* grown on GH26-AcGGM – Mannose 1-6 standards (dashed line), 2-AB labelled
742 GH26-AcGGM (dotted line) and 24 hour supernatant sample (Solid line). A clear increase

743 (upwards arrow) in mannobiose is observed whilst an overall reduction in complexity is also
744 noticeable. Abbreviations: M, mannose; M_2, mannobiose, M_3, mannotriose, M_4,
745 mannotetraose, M_5, mannopentaose, M_6, mannohexaose. **B –** *B. cellulosilyticus* grown on 2-AB
746 labelled GH10-AGX – Xylose 1-6 standards (dashed line), 2-AB labelled GH10-AGX (dotted line)
747 and 24 hour supernatant sample (Solid line). A clear reduction in levels of xylotetraose,
748 xylopentaose and xylohexaose (downwards arrows) was observed whilst an accumulation of
749 xylobiose (upwards arrow) was highly pronounced. Abbreviations: X, xylose X_2, xylobiose; X_3,
750 xylotriose, X_4, xylotetraose; X_5, xylopentaose, X_6, xylohexaose.

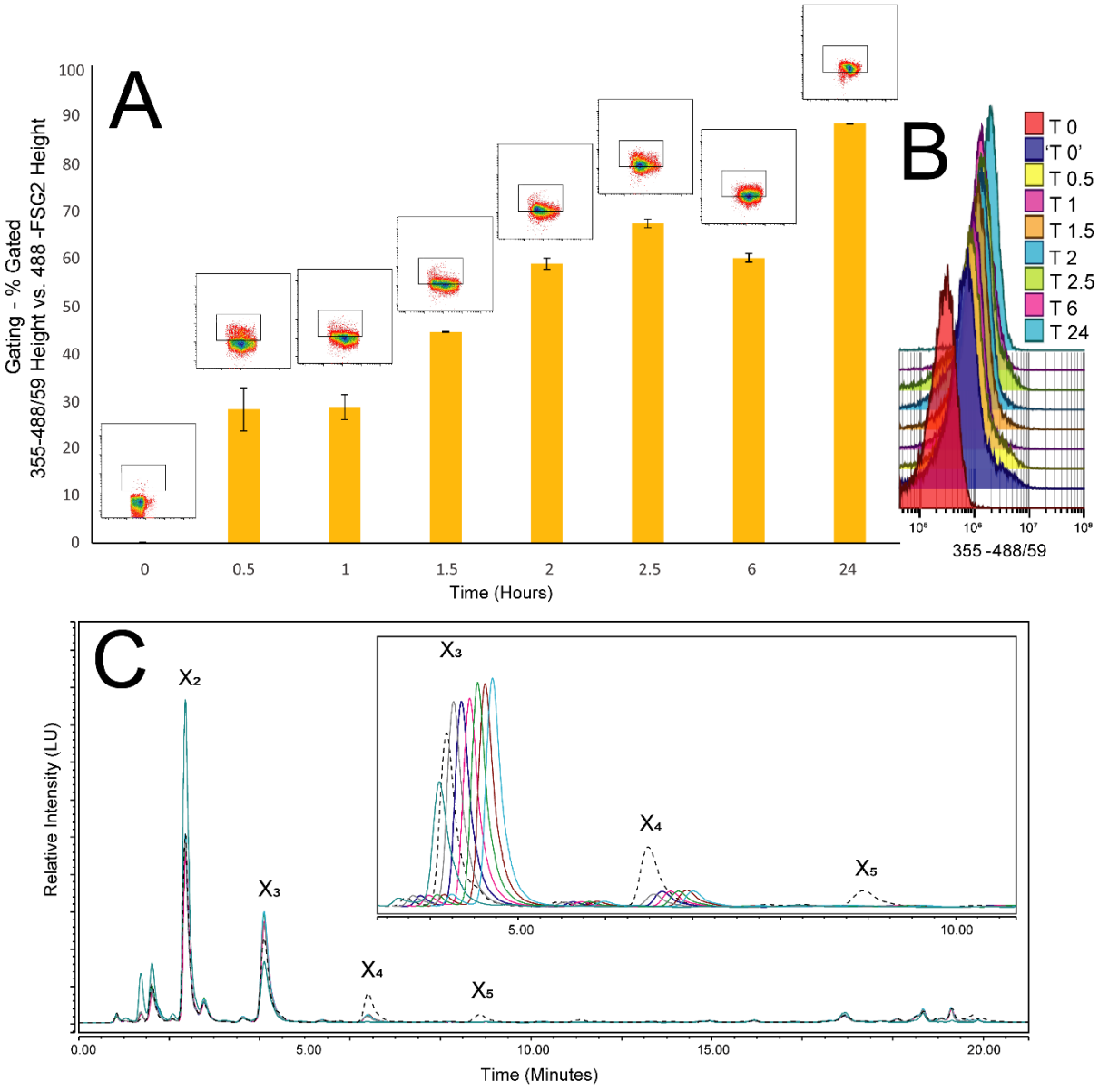

Fig.5 – Monitoring of labelled glycan uptake and degradation over time using a combination of flow cytometry (cell tracking) and HPLC analysis (supernatant tracking) - *B. cellulosilyticus* grown on 2-AB labelled GH10-AGX. **A –** The graph shows an increase in the number of fluorescently labelled cells from flow cytometry measurements (Data based on 2 biological replicates), viewed as a percentage of double positive cells (355 nm/488 nm), through a range of sampling time points, up to 24 hours. **B –** Shift in fluorescence (2-AB 355 nm) at all recorded

758 time points. 'T0' is included as to demonstrate the initial, almost immediate shift that arises
759 from addition of the labelled substrate. **C –** HPLC-HILIC-FLD chromatograms demonstrating the
760 degradation and consumption of the labelled substrate (dotted line) over time on the
761 supernatant of the corresponding cells analysed by flow cytometry – chromatograms are
762 shifted to more clearly show the difference in peak heights. Abbreviations: X_2, xylobiose; X_3,
763 xylotriose, X_4, xylotetraose; X_5, xylopentaose.

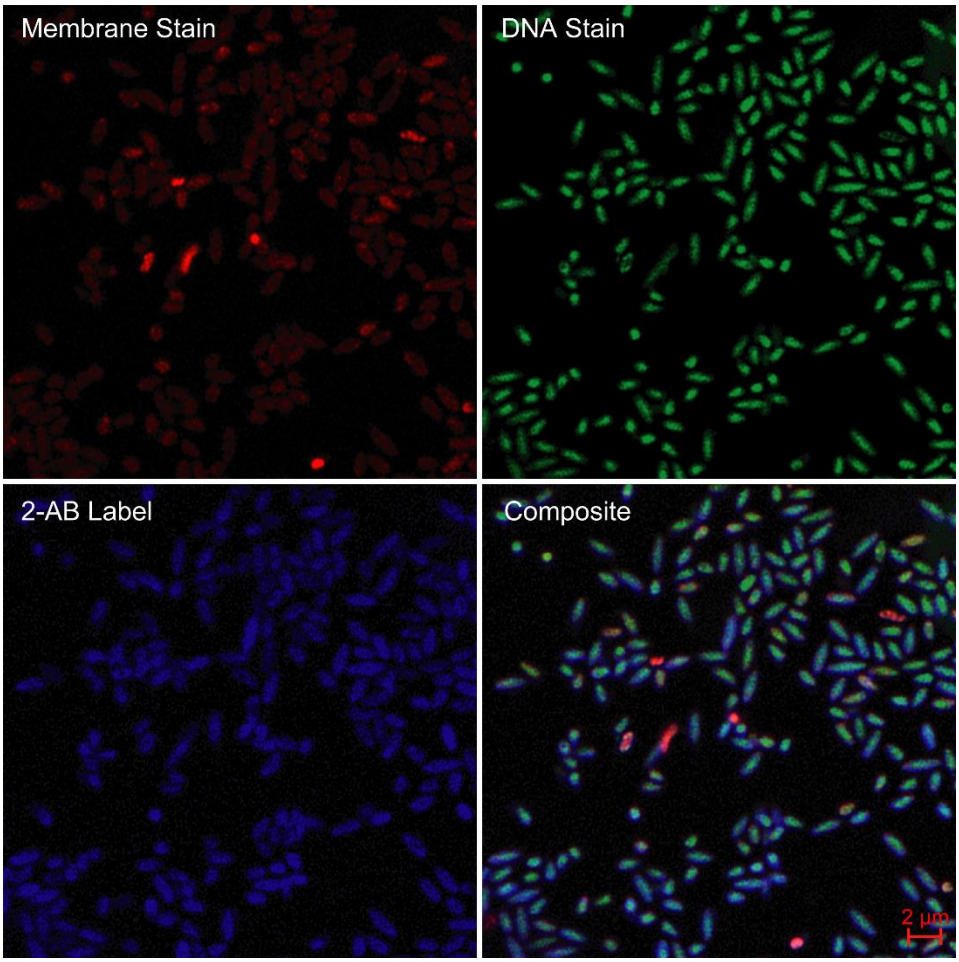

764

765 Fig.6 – Confocal Microscopy of 2-AB labelled cells recovered from *B. cellulosilyticus* grown on
766 GH26-AcGGM after 1 hour. *Top Right* – DNA view of cells stained with SYBR Green I. *Top Left* –

767 Membrane view of cells stained with *Bac*Light Red. *Bottom Left* – View of cells labelled with 2-

768 AB. *Bottom Right* – Composite view of all 3 channels.

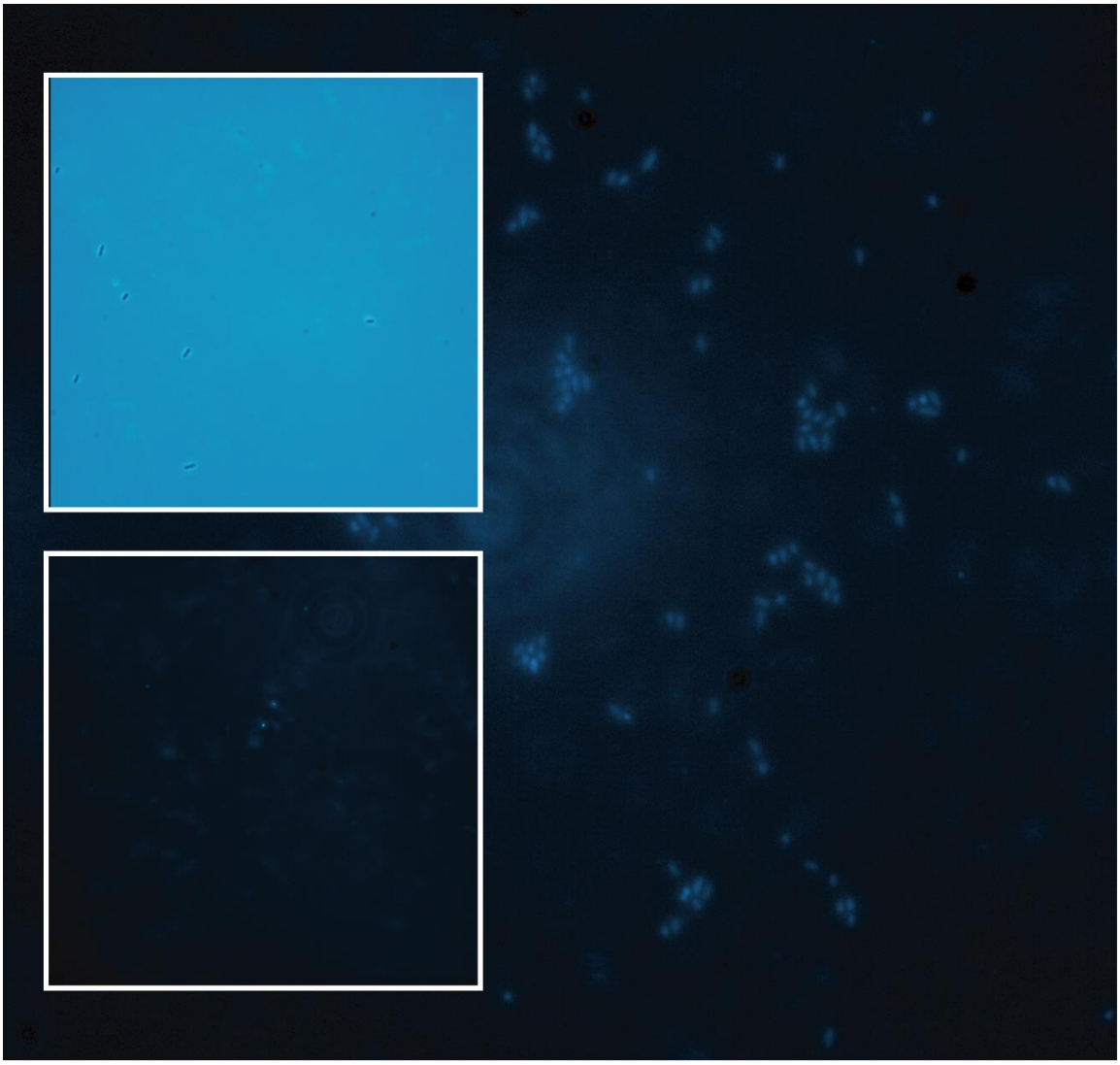

769

770 Fig.7 – Epifluorescence microscopy of 2-AB labelled cells recovered from *B. cellulosilyticus*

771 grown on GH26-AcGGM. *Main Body* – Clusters of 2-AB labelled cells (positive). *Inset Bottom Left*

772 – view of equivalent unlabelled cells (negative). *Inset Top Left* – Brightfield view of equivalent

773 unlabelled cells (negative).

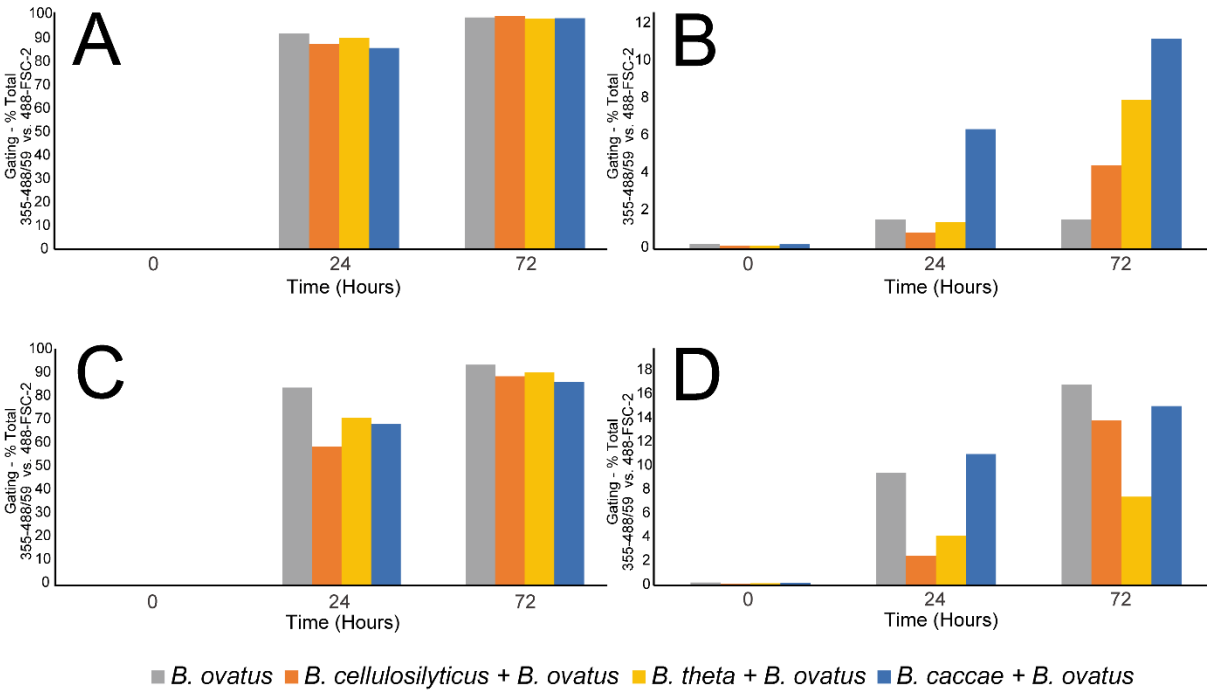

774

775 Fig.8 – Screening of labelled glycan uptake as a function of substrate specificity in co-cultured
776 bacterial fermentations measured by flow cytometry. **A** – AcGGM – Considerable uptake
777 observed after 24 and 72 hours for all strain combinations. **B** – GH26-AcGGM – Comparatively
778 far lower uptake observed after 24 and 72 hours for all strain combinations. **C** – AcAGX –
779 Considerable uptake observed after 24 and 72 hours for all strain combinations. **D** – GH10-AGX
780 – Comparatively far lower uptake observed after 24 and 72 hours for all strain combinations.